Supplement of Geosci. Model Dev., 9, 3671–3684, 2016
http://www.geosci-model-dev.net/9/3671/2016/
doi:10.5194/gmd-9-3671-2016-supplement
© Author(s) 2016. CC Attribution 3.0 License.

Geoscientific Model Development
Open Access
EGU

Supplement of

Computationally efficient air quality forecasting tool: implementation of STOPS v1.5 model into CMAQ v5.0.2 for a prediction of Asian dust

Wonbae Jeon et al.

Correspondence to: Yunsoo Choi (ychoi6@uh.edu)

The copyright of individual parts of the supplement might differ from the CC-BY 3.0 licence.

Table S1. Configuration and detailed physical options for WRF simulation

Number of grids	181 × 143
Horizontal resolution	27 km
Vertical layers	33 layers
Initial data	1°× 1° NCEP Final Operational Global Analysis (FNL)
Microphysics option	WSM 3-class simple ice scheme
Radiation option	RRTM (long wave) / Dudhia (short wave) scheme
Surface layer option	Monin-Obukhov (Janic Eta) scheme
Land-surface option	Unified Noah land-surface model
PBL option	YSU scheme
Cumulus option	Kain-Fritsch (new Eta) scheme

Table S2. Same as Table S1, but for CMAQ

Meteorology	WRF
Number of grids	174 × 128
Horizontal resolution	27 km
Vertical layers	15 layers
Chemical mechanism	CB05 (gas-phase) / AERO6 (aerosol)
Chemical solver	Smvgear
Horizontal advection	Yamo
Horizontal diffusion	Multiscale
Vertical advection	WRF
Vertical diffusion	ACM2
Deposition	M3dry
Anthropogenic emissions	MIX-2010 / CAPSS 2011
Dust emission model	In-line windblown dust model

Table S3. Statistical parameters for the WRF simulation results during the entire simulation period (February 2015) at 20 observational sites. The location of each site is shown in Fig. 2 in the manuscript

Sites	Temperature			Wind Speed		
	RMSE	IOA	MBE	RMSE	IOA	MBE
S1	0.78	0.99	-0.08	1.12	0.97	0.03
S2	1.46	0.98	0.17	1.38	0.90	0.15
S3	2.49	0.90	-0.27	1.23	0.80	-0.85
S4	1.94	0.93	1.80	1.28	0.78	-0.21
S5	2.31	0.93	1.48	1.13	0.84	-0.40
S6	2.31	0.93	1.04	1.89	0.91	1.49
S7	2.48	0.96	-1.46	1.96	0.77	1.43
S8	2.58	0.93	-1.58	1.61	0.87	1.25
S9	1.40	0.94	1.39	1.19	0.86	1.12
S10	1.42	0.95	1.41	1.87	0.91	1.21
S11	2.02	0.97	-1.06	2.03	0.75	1.45
S12	2.70	0.78	-2.35	1.34	0.92	0.94
S13	2.11	0.94	1.24	1.24	0.88	0.85
S14	1.59	0.95	1.01	2.07	0.93	1.46
S15	2.67	0.89	-2.29	2.37	0.76	1.90
S16	1.39	0.98	0.43	1.59	0.89	0.90
S17	2.48	0.84	-1.71	1.98	0.74	1.36
S18	1.60	0.96	-1.09	2.64	0.72	1.27
S19	1.58	0.95	1.17	2.03	0.82	1.02
S20	1.12	0.96	0.98	1.59	0.89	0.90
Average	1.92	0.93	0.01	1.68	0.85	0.86

Table S4. The averaged friction velocity (u_*) in three land cover categories and threshold friction velocity values ($u_{*_{ti,j}}$) for each land cover category used in CMAQ_Dust simulation

Land Cover Categories	u_*	$u_{*_{ti,j}}$ (CMAQ_Dust)
Shrubland	0.23	1.54
Mixed Shrubland-Grassland	0.16	0.55
Barren or Sparsely vegetated	0.18	0.65

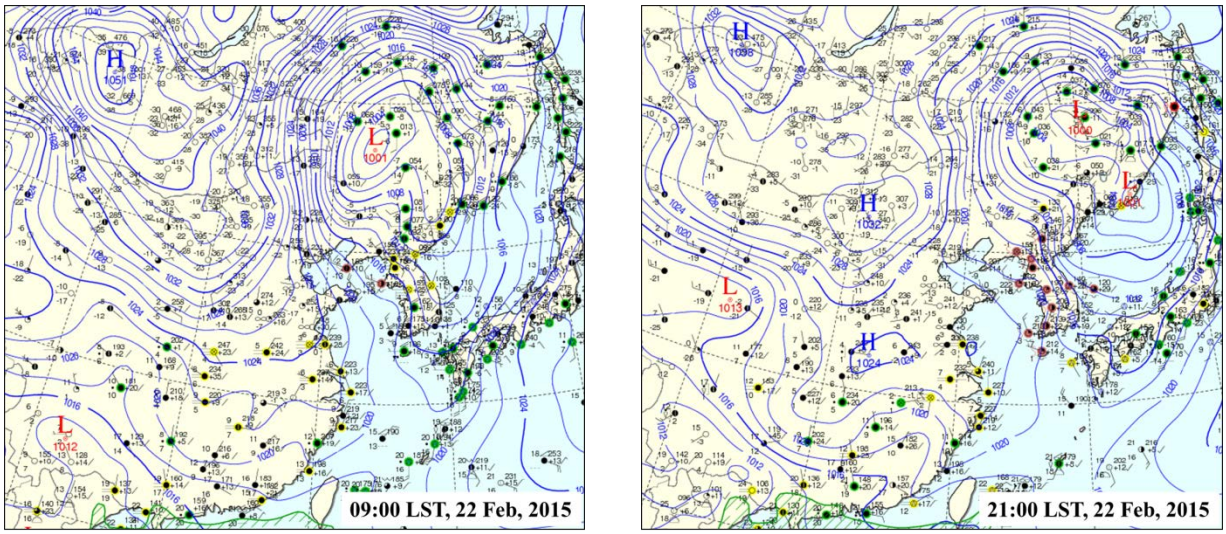

Figure S1. Surface-level synoptic weather chart near the Korean Peninsula on 22 February in 2015, which is the first day of the Asian dust event in this study.

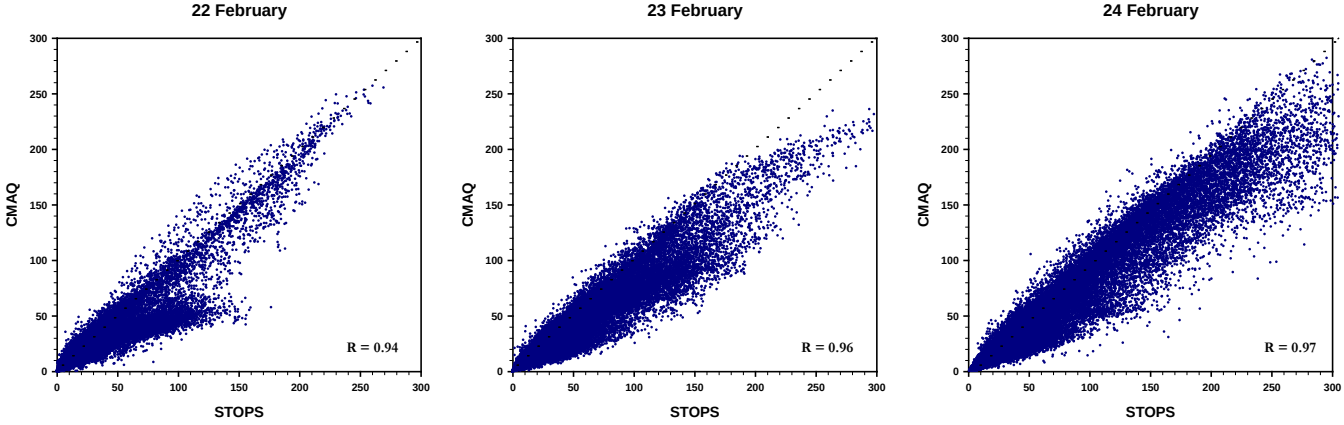

Figure S2. Scatter plots between STOPS- and CMAQ-simulated PM_{10} concentrations during the Asian dust events (22-24 February, 2015). The correlation coefficients (R) appear in the bottom-right of each plot.

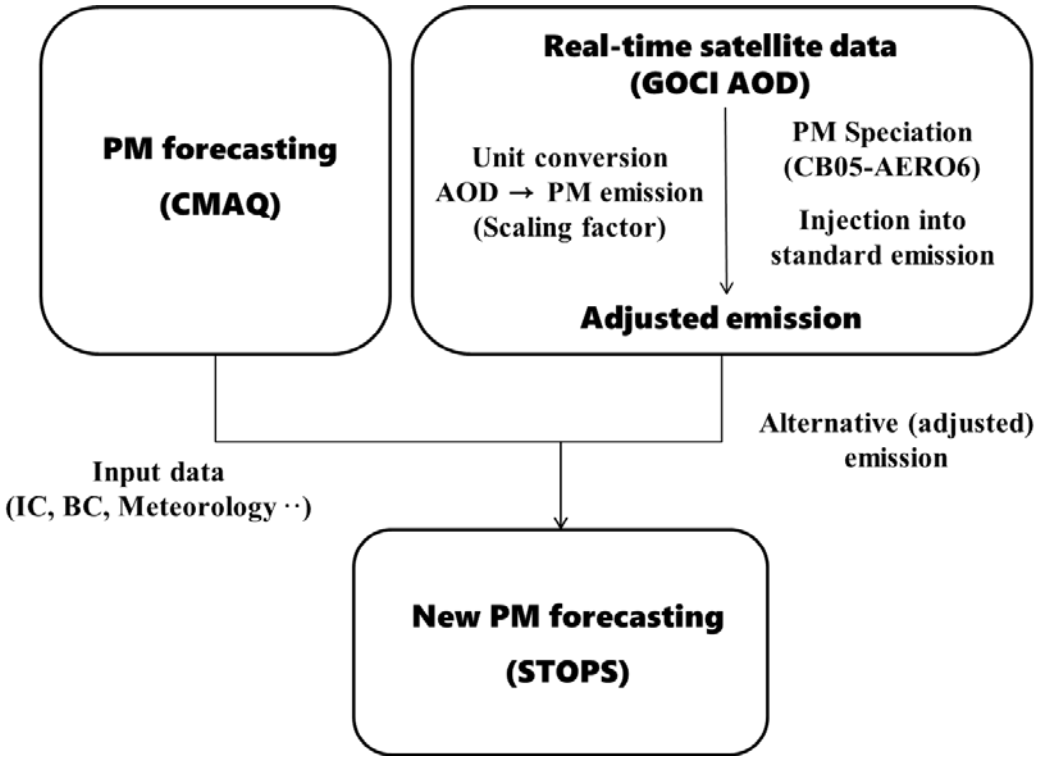

Figure S3. Schematic flowchart describing the procedure of the new PM forecasting using STOPS with the real-time AOD data from GOCI.

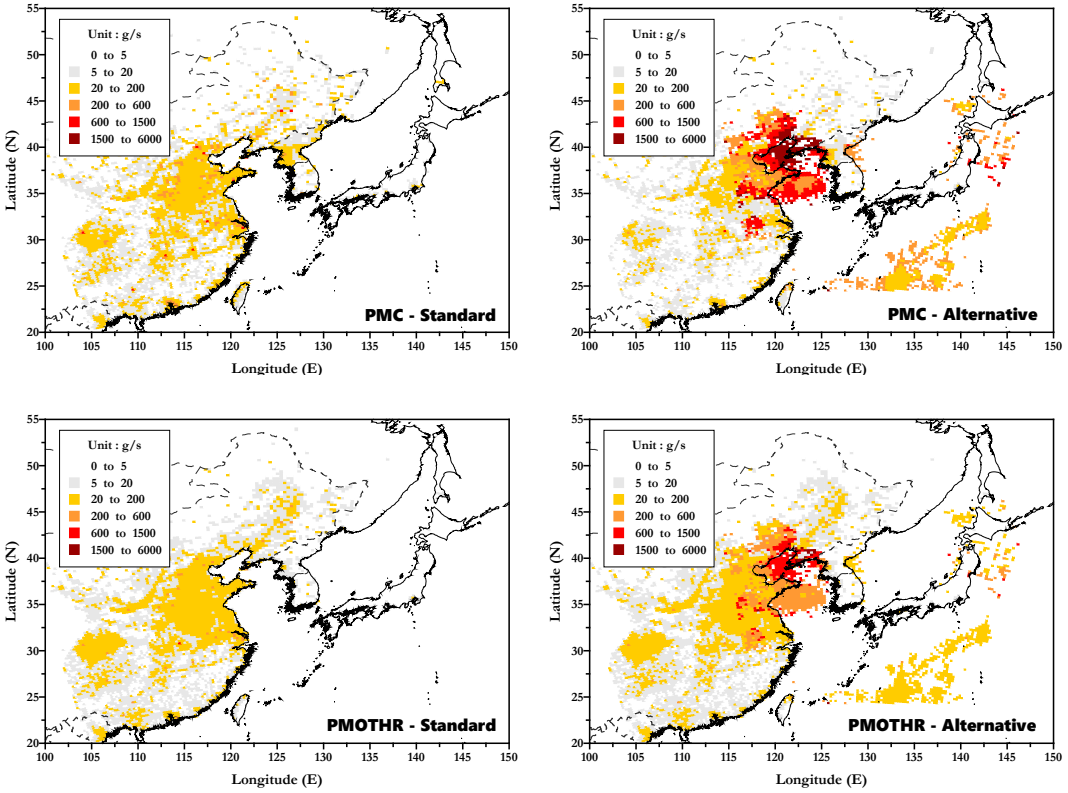

Figure S4. Difference between the emission rates (grams second^{-1}) of standard and alternative emissions (to represent enhanced GOCI AOD) data. The PMC and PMOTHR denote coarse and unspeciated fine particles, respectively.